

Scalar extensions of the SM and recent experimental anomalies

T. Biekötter

*Institute for Theoretical Physics, Karlsruhe Institute of Technology
Wolfgang-Gaede-Str. 1, 76131 Karlsruhe, Germany*

The Brout-Englert-Higgs mechanism describes the generation of masses of fundamental particles in the Standard Model (SM). It predicts the existence of one scalar particle with precisely predicted couplings to fermions and gauge bosons. Deviations from these predictions, such as the observation of additional scalar particles, would indicate non-minimal Higgs sectors and beyond-the-SM physics. We motivate extended scalar sectors based on theoretical and observational grounds and discuss their possible manifestations at colliders or gravitational-wave experiments. We explore smoking-gun signatures of electroweak baryogenesis at the LHC or a future e^+e^- collider, and we examine their interplay with the observation of a primordial gravitational-wave background at LISA. We also consider the possibility of an additional Higgs boson at about 95 GeV motivated by excesses in diphoton and ditau final states observed by CMS. Finally, we discuss the impact of the CDF measurement of the W -boson mass on the parameter space of scalar extensions of the SM.

1 Introduction

The Standard Model (SM) of particle physics has shown remarkable accuracy in predicting observations at high-energy collider experiments, particularly at the Large Hadron Collider (LHC), over a broad range of energy scales. The Brout-Englert-Higgs mechanism^{1,2} of the electroweak (EW) theory describes the generation of particle masses via spontaneous breaking of the EW symmetry. This symmetry breaking results from the non-zero vacuum expectation value (vev) of the Higgs field. The SM incorporates a minimal prescription of EW symmetry-breaking featuring a single scalar $SU(2)$ doublet field. This yields three key predictions which are currently tested at the LHC: (i) the existence of a single scalar particle which, within the current experimental precision, can be identified with the detected Higgs boson at about 125 GeV, denoted h_{125} in the following, (ii) its coupling strengths to massive particles are determined by their masses and they increase with increasing mass, and (iii) no sources of CP violation in the Higgs potential.

Although the SM provides a parametrisation of EW symmetry breaking, it does not describe the underlying physics. Moreover, the SM's Higgs sector faces the problem that the Higgs-boson mass is not protected by a symmetry from larger energy scales and is instead quadratically dependent on any large physical scale present in nature. Thus, a light Higgs boson is considered highly unnatural and not well-understood theoretically.

These shortcomings of the SM can be addressed in beyond the SM (BSM) theories. A wide class of BSM theories feature extended scalar sectors in which additional scalar particles are present at the EW scale. One of the key tasks of the current and future LHC programme is to search for these additional scalar particles to shed light on the physics underlying EW symmetry breaking. Extended scalar sectors also allow for the possibility that the detected Higgs boson is incorporated in such a way that it only approximately resembles a SM Higgs boson. As a

result, the presence of extended Higgs sectors is also probed by the LHC mass and coupling measurements of h_{125} . Given its precisely predicted nature in the SM, h_{125} is an ideal probe of new physics, since any modifications of its signal rates would clearly indicate physics beyond the SM.

The SM has also phenomenological shortcomings that motivate the consideration of extended Higgs sectors. One of the most pressing open issues is the matter-antimatter asymmetry of the universe, which cannot be explained in the SM³. A possible explanation for the observed matter-antimatter asymmetry is EW baryogenesis⁴, where a baryon asymmetry is generated during a first-order EW phase transition through sphaleron processes. However, to render the EW phase transition to be of first order, the SM has to be extended by new degrees of freedom at energy scales close to the EW scale. The addition of BSM scalar fields that themselves could obtain vevs is the most convincing possibility. If the transition is sufficiently strong, the sphalerons are highly suppressed in the EW symmetry breaking phase after the transition such that the previously generated asymmetry cannot be washed out anymore until present times. Given the sizable modifications of the Higgs sector compared to the SM, models that can realize EW baryogenesis can be probed by the LHC, making EW baryogenesis a particularly interesting solution to the unknown origin of the matter-antimatter asymmetry.

A new window to the epoch of the EW phase transition will open once the space-based gravitation wave detector LISA will start taking data. LISA is designed to detect gravitational waves in a frequency band that matches those of the stochastic gravitational wave background as it would be generated during a first-order EW phase transition⁵. Thus, the exploration of the EW scale during the next decades will be marked by the complementarity between the future high-luminosity Runs of the LHC and the LISA experiment.

Upon extending the SM Higgs sector, important experimental restrictions have to be considered. Most importantly, the EW ρ -parameter⁶ defined by $\rho = M_W^2/(\cos^2 \theta_w M_Z^2)$ has been measured experimentally to have a value of $\rho_{\text{exp}} = 1.00038 \pm 0.00020$ ⁷. As a consequence of the custodial symmetry, the SM predicts $\rho = 1$ at the classical level, in remarkable agreement with ρ_{exp} . If one adds additional EW multiplets to the Higgs sector of the SM, the prediction for the ρ -parameter is in general different from one. It is therefore convincing to study models in which $\rho \approx 1$ holds without fine tuning of the model parameters, such that the experimentally measured value is not just a strange coincidence. It turns out that the addition of only gauge singlet scalar fields and SU(2) doublet fields maintains the SM prediction $\rho = 1$ at the classical level. We will therefore focus in the following on the two Higgs doublet model (2HDM) and the singlet-extended 2HDM (S2HDM).

2 The (singlet-extended) two Higgs doublet model

The two Higgs doublet model (2HDM) contains two scalar SU(2) doublet fields Φ_1 and Φ_2 ⁸. Neglecting sources of CP violation, and assuming the presence of a softly broken Z_2 symmetry under which one of the doublet fields changes its sign, the scalar potential can be written as

$$V_{2\text{HDM}} = m_{11}^2 |\Phi_1|^2 + m_{22}^2 |\Phi_2|^2 - m_{12}^2 (\Phi_1^\dagger \Phi_2 + \text{h.c.}) + \frac{\lambda_1}{2} (\Phi_1^\dagger \Phi_1)^2 + \frac{\lambda_2}{2} (\Phi_2^\dagger \Phi_2)^2 + \lambda_3 (\Phi_1^\dagger \Phi_1) (\Phi_2^\dagger \Phi_2) + \lambda_4 (\Phi_1^\dagger \Phi_2) (\Phi_2^\dagger \Phi_1) + \frac{\lambda_5}{2} [(\Phi_1^\dagger \Phi_2)^2 + \text{h.c.}] . \quad (1)$$

The Z_2 symmetry can be extended to the Yukawa sector, where as a result of the opposite Z_2 parities the scalar doublets cannot be coupled both to the same fermion. This leads to the absence of flavour-changing neutral currents at classical level in agreement with experimental observations. Depending on the different possibilities for assigning Z_2 parities to the different kind of fermions, one finds the four different Yukawa types I, II, III (lepton-specific) and IV (flipped).

The two Higgs doublets have a total of eight degrees of freedom, from which three belong to the Goldstone bosons after EW symmetry breaking and are thus absorbed into the longitudinal

degrees of freedom of the massive gauge bosons W^\pm and Z . The remaining degrees of freedom give rise to five physical scalar states: two scalar states h and H , where in the following h is assumed to be the lighter state, and which plays the role of the detected Higgs boson at 125 GeV, a pseudoscalar state A , and a pair of charged Higgs bosons H^\pm . The mixing of h and H is commonly expressed in terms of the mixing angle α . In the *alignment limit* $\cos(\beta - \alpha) = 0$, where the parameter β is defined by $\tan \beta = v_2/v_1$, the couplings of the state h are equal to the couplings of a SM Higgs boson.

Extending upon the 2HDM, the singlet extended 2HDM (S2HDM) adds an additional complex scalar field Φ_S acting as a singlet under the gauge symmetries. We will consider a variation of the model in which Φ_S transforms under an additional global U(1) symmetry, whereas all other fields are invariant under this symmetry⁹. We furthermore assume the spontaneous breaking of the U(1) symmetry by means of a non-zero vev v_S of the singlet field. To avoid the presence of a massless mode as a Goldstone boson associated with this symmetry breaking, we assume the presence of a bilinear U(1)-breaking term in the potential. Accordingly, the scalar potential can be written as

$$V_{\text{S2HDM}} = V_{\text{2HDM}} + \frac{1}{2}m_S^2|\Phi_S|^2 + \frac{\lambda_6}{2}|\Phi_S|^4 + \frac{\lambda_7}{2}|\Phi_1|^2|\Phi_S|^2 + \frac{\lambda_8}{2}|\Phi_2|^2|\Phi_S|^2 - \frac{\mu_\chi^2}{4}(\Phi_S^2 + \text{h.c.}) , \quad (2)$$

where the terms proportional to μ_χ^2 softly break the global U(1) symmetry. As before, the invariance under the discrete Z_2 acting on Φ_1 and Φ_2 was imposed to suppress tree-level flavour-changing neutral currents.

The S2HDM has two additional physical scalar states in comparison to the 2HDM. The real component of Φ_S mixes with the neutral real components of Φ_1 and Φ_2 , forming a total of three CP-even Higgs bosons $h_{1,2,3}$. The imaginary component of Φ_S gives rise to a massive stable scalar state χ that can act as a dark-matter candidate in the form of pseudo-Nambu-Goldstone dark matter. This form of Higgs-portal dark matter gained attention in recent years since the cross sections for the scattering of χ on nuclei are vanishing at classical level due to a cancellation mechanism resulting from the global U(1) symmetry. As a result, the S2HDM passes constraints from dark-matter direct-detection experiments without a tuning of parameters¹⁰. In total analogy to the 2HDM, the scalar spectrum contains the pseudoscalar state A and the charged Higgs bosons H^\pm .

3 Experimental opportunities

As already mentioned above, so far no clear hints for extended scalar sectors (or any other kind of BSM physics) have been observed at the LHC. In the following, I will discuss several possibilities for which the presence of an extended Higgs sector could still reveal itself in the near future at the LHC. I will also discuss the possible interplay with other experiments, such as the LISA experiment, either in order to further constrain the parameter space of BSM theories, or in order to discriminate between different BSM theories if evidence for BSM physics will be found in the near future.

3.1 Smoking-gun signals of electroweak baryogenesis

Under the presence of a second Higgs doublet, it is possible to render the EW phase transition to be of strongly first-order, which is a vital ingredient for the realization of EW baryogenesis. In the type II 2HDM, the most promising scenario for the realization of a first-order phase transition is characterized by the mass hierarchy $m_H \ll m_A \approx m_{H^\pm}$. Due to the mass splitting between H and A , the process $A \rightarrow ZH$ has been coined as a smoking-gun signature of EW baryogenesis in the 2HDM¹¹. Both ATLAS and CMS have searched for this signature assuming that H decays into bottom-quark or tau-lepton pairs. In Ref.¹² we have shown that as a consequence of the existing constraints on the type II 2HDM, H tends to be so heavy that it is predicted

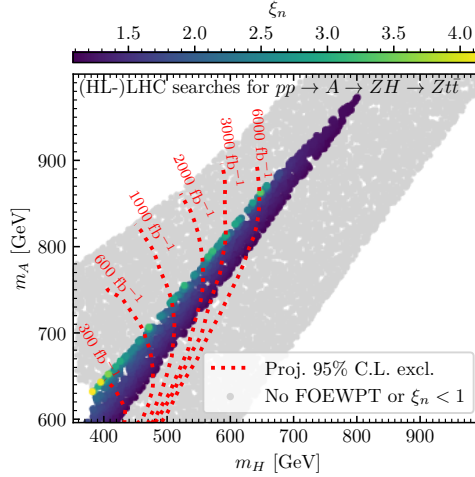


Figure 1 – The (m_H, m_A) plane in the type II 2HDM for $\tan\beta = 3$, $\cos(\alpha - \beta) = 1$, and $m_{12}^2 = m_H^2 \sin\beta \cos\beta$, with the color coding indicating the value of ξ_n if $\xi_n > 1$. The remaining points are shown in grey. The red dashed lines indicate the projected 95% confidence-level exclusion regions resulting from the (HL-)LHC searches for the process $pp \rightarrow A \rightarrow ZH$ with H decaying into a pair of top quarks. Taken from Ref. ¹².

to dominantly decay into top-quark pairs. Notably, results for the search for the smoking-gun signature in $Zt\bar{t}$ final states has not been published yet, but efforts to analyze such final states are ongoing by both ATLAS and CMS.

In Fig. 1 we show the results of a scan in the alignment limit of the type II 2HDM for $\tan\beta = 3$ ¹². Here the parameter points featuring a strong first-order phase transition are indicated with the colors. The color coding indicates the value of $\xi_n = v_n/T_n$, where v_n and T_n are the vev v and the temperature T at the transition, respectively, and where a strong transition is defined by $\xi_n > 1$, as such transition prevents any washout of the baryon asymmetry. The remaining points are shown in grey. We also show the expected 95% confidence-level exclusion sensitivity for different values of the integrated luminosity \mathcal{L} . These were obtained from a naive rescaling of expected CMS limits assuming $\mathcal{L} = 41 \text{ fb}^{-1}$ (see Ref. ¹² for details). Comparing the red dashed lines to the region in which a first-order phase transition can be realized, one can see that the LHC will have a significant discovery potential, in particular during its high-luminosity phase. On the other hand, if no deviations from the SM background expectation will be found, large parts of the 2HDM parameter regions suitable for EW baryogenesis would be excluded. Here it should be taken into account that the gluon-fusion production cross section of A scales with $1/(\tan\beta)^2$, such that for smaller values of $\tan\beta$, as preferred for a realization of EW baryogenesis, the experimental prospects are even better.^a

A first-order EW phase transition in the 2HDM is not only associated with BSM Higgs bosons not much heavier than the EW scale, but it is also linked to sizable modifications of the trilinear self-coupling of $h = h_{125}$. This modifications are usually expressed in terms of the parameter $\kappa_\lambda = \lambda_{hhh}/\lambda_{hhh}^{\text{SM}}$, where λ_{hhh} is the 2HDM coupling prediction, and $\lambda_{hhh}^{\text{SM}}$ is the tree-level Higgs boson self-coupling in the SM. In Fig. 2, in which we depict the predictions for κ_λ against the signal-to-noise ratio (SNR) at LISA for the detection of the primordial gravitational-wave background as it would have been generated during the phase transition ¹². We only show here the predictions for the subset of parameter points shown in Fig. 1 for which the SNR is of the order of one or larger, i.e. for parameter points that feature a gravitational-wave signal that potentially is detectable at LISA.^b One can see that these points predict $\kappa_\lambda \approx 2$. The LHC is expected to be able to disfavour such values of κ_λ at the level of 2σ if no deviations from

^aWe note that the measurement of the cross section for this signature might reveal important information about the underlying model that is realized in nature. For instance, possible ways to distinguish between a 2HDM and an S2HDM realization by means of the $A \rightarrow ZH$ signature have been discussed in Ref. ¹³.

^bSee Ref. ¹² for details on the prediction of the gravitational-wave signals.

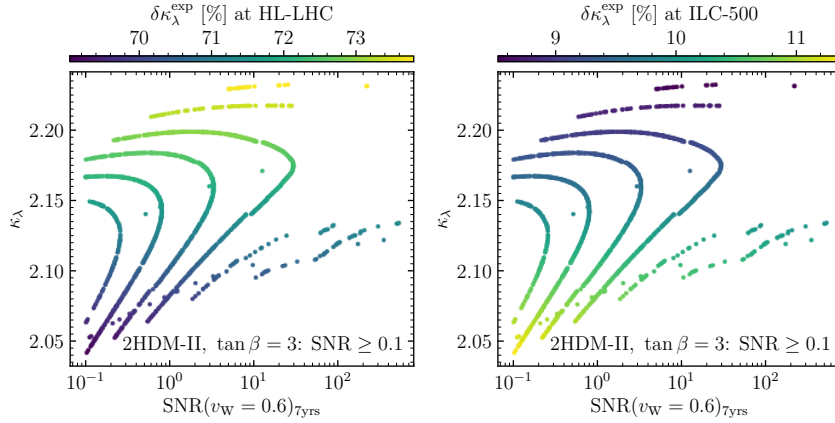


Figure 2 – 2HDM type II parameter points with $\text{SNR} \geq 0.1$ in the $(\text{SNR}, \kappa_\lambda)$ plane. The color coding of the points indicates the projected experimental precision of the measurement of κ_λ at the HL-LHC (left) and the ILC-500 (right), see text for details. Taken from Ref. ¹².

the SM expectations for the non-resonant pair-production of h_{125} will be found during the high-luminosity phase¹⁴. Here one should note that the destructive interference between the s -channel and the box diagram leads to a smaller LHC cross section for the pair-production of h_{125} for values of $\kappa_\lambda \approx 2$ compared to the SM prediction. As a result, assuming that $\kappa_\lambda \approx 2$ is realized in nature, the relative precision with which κ_λ could be determined at the LHC (indicated with the colors of the points in the left plot of Fig. 2) is only about 70%. As a comparison, the expected precision on $\kappa_\lambda \approx 1$, i.e. assuming SM cross sections for h_{125} -pair production, is 60%. In the right plot of Fig. 2, the color coding indicates the relative precision of a measurement of κ_λ at the International Linear Collider (ILC) operating at $\sqrt{s} = 500$ GeV. One can see that an e^+e^- collider with sufficient energy to pair-produce h_{125} could improve substantially the experimental precision with which κ_λ -values of about two could be determined.

The results discussed in this section demonstrate that the Higgs measurements at the LHC in the upcoming years will shape in a profound way the expectations for the possibility of measuring a gravitation-wave background produced during a first-order EW phase transition at LISA. In the hypothetical scenario in which no additional Higgs bosons will be found, and in which the coupling measurements of the detected Higgs boson will show no indications of BSM physics, the LHC will limit the possibility of detecting a primordial gravitational-wave background as a remnant of the EW phase transition to corners of the parameter space of many models.

3.2 A Higgs boson at 95 GeV?

Many phenomenological analyses of models with extended scalar sectors focus on scenarios in which h_{125} is the lightest Higgs boson. However, additional Higgs bosons lighter than 125 GeV are still experimentally viable if their couplings to gauge bosons are suppressed compared to the ones of a SM Higgs boson, for instance due to a large singlet admixture.

In view of this, it is interesting that several local excesses have been observed at a mass of about 95 GeV: (i) LEP observed an excess in $e^+e^- \rightarrow ZH$ with H decaying into bottom-quark pairs (2.3σ local significance)¹⁵. (ii) CMS observed an excess in $pp \rightarrow H \rightarrow \tau^+\tau^-$ using the full Run 2 dataset (3.1σ local significance)¹⁶. (iii) CMS observed an excess in $pp \rightarrow H \rightarrow \gamma\gamma$ in the 8 TeV dataset (2σ local significance)¹⁷ and in the 13 TeV dataset (2.9σ local significance)^{18,19}. The latter diphoton excess at 13 TeV was reported previously based only on the first-year Run 2 dataset¹⁸. During the Moriond conference, the updated result including the full Run 2 data was presented²⁰, showing a practically unchanged significance of the excess, but the excess corresponds to a smaller signal rate as compared to the previous result. It should be noted that, in addition to the inclusion of more data, the updated result¹⁹ also has a refined experimental

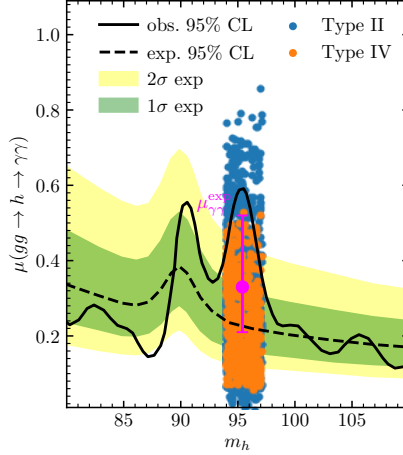


Figure 3 – S2HDM parameter points passing the applied constraints in the $(m_{h_{95}}, \mu_{\gamma\gamma})$ for the type II (blue) and the type IV (orange). The expected and observed cross section limits obtained by CMS are indicated by the black dashed and solid lines, respectively, and the 1σ and 2σ uncertainty intervals are indicated by the green and yellow bands, respectively. The value of $\mu_{\gamma\gamma}^{\text{exp}}$ and its uncertainty is shown with the magenta error bar at the mass value at which the excess is most pronounced. Taken from Ref. ²¹.

analysis for the background rejection of misidentified $Z \rightarrow e^+e^-$ Drell-Yan events, and further event classes requiring additional jets have been utilized. Taking this into account, from our point of view, the persistence of the diphoton excess strengthens the motivation to investigate a BSM interpretation of the excesses.

In Ref. ²¹ we have investigated whether the S2HDM can accommodate the excesses by means of a singlet-like scalar at 95 GeV whose couplings to the fermions and gauge bosons result from the mixing with h_{125} . As shown in Fig. 3, both type II and type IV (flipped) can give rise to a state that describes the CMS diphoton excess, while being in agreement with all relevant theoretical and experimental constraints. In our previous studies ^{22,9,23,24}, in which a signal rate for the diphoton excess of $\mu_{\gamma\gamma}^{\text{exp}} = 0.6 \pm 0.2$ based on the earlier CMS analysis including only the first-year Run 2 dataset was considered ¹⁸, we found a preference for type II, in which larger diphoton signal rates can be achieved. The updated value ²⁰ of $\mu_{\gamma\gamma}^{\text{exp}} = 0.33^{+0.19}_{-0.12}$ is such that both type II and type IV can describe the diphoton excess equally well. General implications of the reduction of $\mu_{\gamma\gamma}^{\text{exp}}$ for an interpretations in different classes of BSM theories are discussed in Ref. ²¹.

We have also analysed whether the other excesses at about 95 GeV can be described in addition to the diphoton excess. We have shown that both type II and type IV can additionally accommodate the LEP excess, however only in type IV also a sizable signal for the CMS ditau excess can be achieved. However, even in type IV the ditau excess can only be described at the level of 1σ due to constraints from a related CMS search for $pp \rightarrow ttH$ with $H \rightarrow \tau^+\tau^-$ ²⁵, in which no excess has been observed at and around 95 GeV.

3.3 The CDF W -boson mass measurement and isospin splitting

The SM does not predict the masses of the fundamental particles. However, one can find relations between the masses and other measured quantities. The mass of the W boson M_W can be expressed from muon decay as a function of the Fermi constant G_μ , the fine structure constant α , and the masses of the Z boson via the relation

$$M_W^2 = M_Z^2 \left(\frac{1}{2} + \sqrt{\frac{1}{4} - \frac{\alpha\pi}{\sqrt{2}G_\mu M_Z^2}(1 + \Delta r)} \right). \quad (3)$$

Here, the parameter Δr incorporates the quantum corrections, which in the SM have been evaluated up to four-loop order. It is important to note that the leading order prediction for

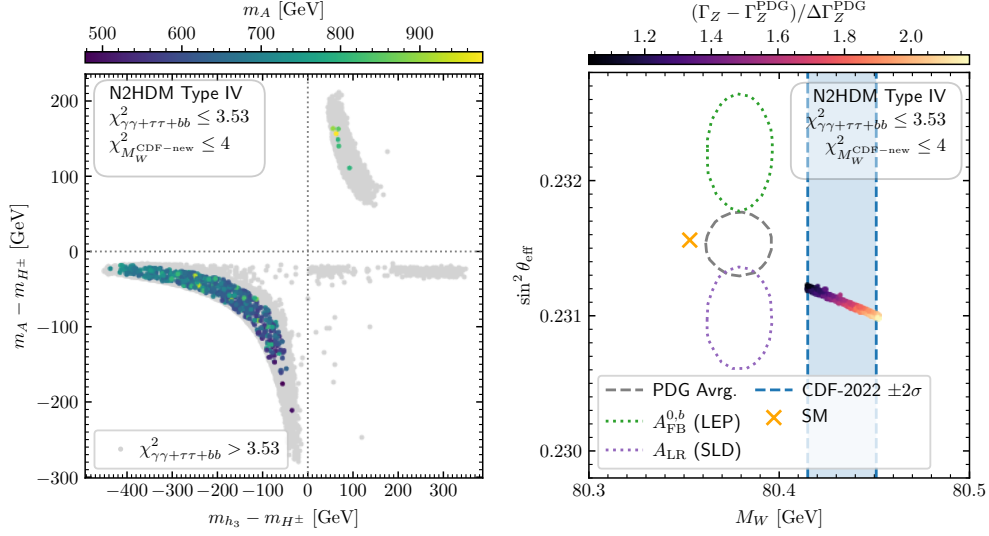


Figure 4 – Left: S2HDM parameter points that predict a value of M_W within the 2σ uncertainty band of the CDF measurement in the plane of the mass differences $m_{h_3} - m_{H^\pm}$ and $m_A - m_{H^\pm}$. The color coding indicates the value of m_A for the parameter points that describe the excesses at 95 GeV at the level of 1σ or better. The remaining parameter points, are shown in gray. Right: The predictions for M_W and $\sin^2 \theta_{eff}$ in the S2HDM. The color coding of the points indicates the difference between the prediction for Γ_Z and the PDG average value Γ_Z^{PDG} divided by the experimental uncertainty $\Delta\Gamma_Z^{PDG}$. The light blue region corresponds to the new CDF measurement within $\pm 2\sigma$. The violet and the green dotted ellipses indicate the 68% confidence level limits from the two individually most precise measurements of $\sin^2 \theta_{eff}$ via $A_{FB}^{0,b}$ at LEP and A_{LR} at SLD, respectively, whereas the gray dashed ellipse indicates the PDG average. The orange cross indicates the SM prediction. Both plots taken from Ref. ²⁴.

M_W in the SM is in large disagreement with the experimentally measured value, and only the inclusion of the quantum corrections shift the prediction to larger values in agreement with the 2022 PDG average value. One of the most important corrections contained in $\Delta\rho$ is given by the EW $\Delta\rho$ -parameter which quantifies the breaking of the custodial symmetry (see the discussion in Ref. 1). In the SM, the most important corrections contained in $\Delta\rho$ result from the isospin splitting in the fermion sector, where due to the large mass splitting between top quark and bottom quark one finds the approximate proportionality $\Delta\rho \sim (m_t^2 - m_b^2)$.

In the year 2022 the CDF collaboration has published a new measurement of the W -boson mass utilizing an integrated luminosity of 8.8 fb^{-1} collected at the Tevatron $p\bar{p}$ collider. The result was $M_W^{CDF} = 80.4335 \pm 0.0094 \text{ GeV}$, which deviates from the SM prediction for M_W by about 7σ . However, one should have in mind that the CDF measurement is not only in disagreement with the SM, but also with all previous measurements of M_W at LEP, the Tevatron and the LHC. At this moment in time, one cannot disregard neither the CDF measurement (being the most precise one) nor the previous measurements of M_W (being consistent within each other and with the SM).^c

Nevertheless, given the large discrepancy with the SM, one can ask the question whether there are models with extended scalar sectors which could accommodate a sizable upwards shift to M_W , even as large as the CDF result, without being in tension with other observables. Scalar extensions with a second SU(2) Higgs doublet are promising candidates, since the additional BSM scalars can give rise to additional sources of isospin splitting. In the 2HDM, one finds at the one-loop level that $\Delta\rho \sim (m_A^2 - m_{H^\pm}^2)(m_H^2 - m_{H^\pm}^2)$, i.e. an upwards shift to the prediction for M_W requires the pseudoscalar A and the heavy scalar H to be both lighter or both heavier than the charged scalars H^\pm . In Ref. ²⁴ we exploited this feature in order to simultaneously accommodate the CDF M_W measurement and the collider excesses at 95 GeV in the S2HDM, see left plot of Fig. 4. In the right plot of Fig. 4 one can see that in this case also the prediction

^cThe ATLAS collaboration reported an update on their M_W determination during this year's Moriond EW conference ²⁶, where an improved statistical interpretation was applied, showing good agreement with the SM.

for the effective weak mixing angle $\sin^2 \theta_{\text{eff}}$ is affected, making it more compatible with the SLD measurement of A_{LR} , but less so with the LEP measurement of $A_{\text{FB}}^{0,b}$. No significant tension for the width of the Z boson Γ_Z is found.

4 Conclusions

After the discovery of a SM-like Higgs boson at 125 GeV, a prime goal of the current and future LHC science programme is to shed more light on the physics underlying EW symmetry breaking. No clear evidence for physics beyond the SM has been found yet, but models with extended Higgs sectors are well motivated candidates. Here we discussed several measurements by which the presence of an extended Higgs sector might reveal itself in the near future.

Acknowledgments

I thank my collaborators with whom the results reviewed here have been obtained: P. Gabriel, S. Heinemeyer, M.O. Olea Romacho, J.M. No, R. Santos and G. Weiglein. I furthermore thank M.O. Olea Romacho for valuable comments during the preparation of my talk. I am grateful to the organizers of the Moriond conference for the kind invitation, the welcoming atmosphere during the conference, and for giving me the opportunity to present my work. This work is supported by the German Bundesministerium für Bildung und Forschung (BMBF, Federal Ministry of Education and Research) – project 05H21VKCCA.

References

1. F. Englert and R. Brout. *Phys. Rev. Lett.*, 13:321–323, 1964.
2. P. W. Higgs. *Phys. Rev. Lett.*, 13:508–509, 1964.
3. K. Kajantie, M. Laine, K. Rummukainen, et al. *Phys. Rev. Lett.*, 77:2887–2890, 1996.
4. V. A. Kuzmin, V. A. Rubakov, and M. E. Shaposhnikov. *Phys. Lett. B*, 155:36, 1985.
5. LISA Cosmology Working Group. *astro-ph/2204.05434*, 2022.
6. D. A. Ross and M. J. G. Veltman. *Nucl. Phys. B*, 95:135–147, 1975.
7. R. L. Workman et al. Review of Particle Physics. *PTEP*, 2022:083C01, 2022.
8. T. D. Lee. *Phys. Rev. D*, 8:1226–1239, 1973.
9. T. Biekötter and M. O. Olea-Romacho. *JHEP*, 10:215, 2021.
10. T. Biekötter, P. Gabriel, M. O. Olea-Romacho, et al. *JHEP*, 10:126, 2022.
11. G. C. Dorsch, S. J. Huber, K. Mimasu, et al. *Phys. Rev. Lett.*, 113(21):211802, 2014.
12. T. Biekötter, S. Heinemeyer, J. M. No, et al. *JCAP*, 03:031, 2023.
13. T. Biekötter, S. Heinemeyer, J. M. No, et al. *JCAP*, 06:018, 2021.
14. ATLAS collaboration. *ATL-PHYS-PUB-2022-018*, 2022.
15. R. Barate et al. *Phys. Lett. B*, 565:61–75, 2003.
16. CMS collaboration. *hep-ex/2208.02717*, 2022.
17. CMS collaboration. *CMS-PAS-HIG-14-037*, 2015.
18. CMS collaboration. *Phys. Lett. B*, 793:320–347, 2019.
19. CMS collaboration. *CMS-HIG-20-002*, 2023.
20. S. Gascon-Shotkin. On behalf of CMS collab., *Talk at Rencontres de Moriond EW*, 2023.
21. T. Biekötter, S. Heinemeyer, and G. Weiglein. *hep-ph/2303.12018*, 2023.
22. T. Biekötter, M. Chakraborti, and S. Heinemeyer. *Eur. Phys. J. C*, 80(1):2, 2020.
23. T. Biekötter, S. Heinemeyer, and G. Weiglein. *JHEP*, 08:201, 2022.
24. T. Biekötter, S. Heinemeyer, and G. Weiglein. *hep-ph/2204.05975*, 2022.
25. CMS collaboration. *CMS-PAS-EXO-21-018*, 2022.
26. ATLAS collaboration. *ATLAS-CONF-2023-004*, 2023.